Processing of AlSi13Mg5 foams using Mg and AlMg50 blowing agents

K. Georgy[1,2,3]*, C. E. Jiménez[3,4,5], F. García-Moreno[3,4], M. Mukherjee[1,2]

[1]*Metal Foams and Porous Materials Lab, Department of Metallurgical and Materials Engineering, Indian Institute of Technology Madras, Chennai 600036, India*

[2]*Applied Magnesium Research Group - Centre of Excellence in Materials and Manufacturing for Futuristic Mobility, Indian Institute of Technology Madras, Chennai 600036, India*

[3]*Institute of Materials Science and Technology, Technische Universität Berlin, Hardenbergstraße 36, 10623, Berlin, Germany*

[4]*Institute of Applied Materials, Helmholtz-Zentrum Berlin für Materialien und Energie, Hahn-Meitner Platz 1, 14109 Berlin, Germany*

[5]*Dept. Interface Design, Helmholtz-Zentrum Berlin für Materialien und Energie GmbH (HZB), Albert-Einstein-Str.15, 12489, Berlin, Germany*

* Correspondence: georgykuriank@gmail.com, Phone: +91–9164845785

Keywords: Metal foam, powder metallurgy, mechanical properties, blowing agent

Abstract

Aluminium closed-cell foams with superior structure and properties can be produced using Mg-based blowing agents. In this study, AlSi13Mg5 foams were produced via the powder metallurgy route using two different Mg-based blowing agents: Pure Mg powders and pre-alloyed AlMg50 powders. Mass spectrometry was performed to determine their hydrogen desorption characteristics. In Mg powder, the peak gas release occurred at 364 °C compared to the delayed peak gas release at 420 °C from AlMg50 powder. The structure and properties of the foams produced using these two blowing agents were compared by performing image

analysis and compression tests, respectively. Peak strength of foams produced using Mg powder is 7.3 ± 0.6 MPa and BA-AM foam is 8 ± 0.4 MPa.

1. Introduction

Metal foams are used in many structural and functional applications [1,2]. Various blowing agents have been exploited so far for their fabrication [3–6]. Different types of modifications are performed to some of these blowing agents to tailor their gas releasing behaviour, which is essential for improving the quality of the foams [7–10]. Mg-based blowing agents (Mg, AlMg50, etc.) play a dual role in the production of metal foams: They act i) as the source of Mg, which is a targeted alloying element, and ii) as the intrinsic gas source that provides the gas required for foaming. Al-based foams produced using Mg-based blowing agents possess uniform structure with fewer defects [11,12]. Alloying with Mg also improves the yield strength of the matrix [13,14]. Because of these reasons, the foams produced using Mg-based blowing agents exhibit higher strength than the foams produced using conventional blowing agents such as metal hydrides or carbonates. Use of Mg as blowing agent also eliminates the presence of unwanted alloying elements resulted from conventional blowing agent, for example, Ti from TiH_2 [15]. Among the few alloys investigated where Mg blowing agent was used, Al-Si-Mg alloy foams exhibited the highest burning and corrosion resistance [13]. In this alloy system, AlSi13Mg5 alloy foams showed the most favourable properties [14], which can be improved further by age hardening [16]. Therefore, AlSi13Mg5 alloy foamed using Mg blowing agent is a promising system for commercial production of metal foams.

Barode et al. used different Mg-based blowing agents to foam AlMg15Cu10 alloy and demonstrated that AlMg50 powder is a better blowing agent compared to Mg powder [12]. However, their study was limited only to AlMg15Cu10 alloy foam. AlMg15Cu10 foams are less favoured for applications because they are relatively brittle, exhibit less corrosion resistance and they also contain the heavier element Cu [13]. Since AlSi13Mg5 alloy foam has the potential for commercialization, it is imperative to identify an appropriate source of Mg for this alloy. As Mg and AlMg50 powders are commercially available, these powders were used in the present study. The objective of the present study is to exploit both Mg and AlMg50 blowing agents to produce AlSi13Mg5 alloy foams and to identify which blowing agent results in better structure and property. Since Mg is easily prone to catch fire, hence identifying an alternative gas source for foaming would be beneficial in some of the applications.

2. Materials and methods

Al (Alfa Aesar, 99.5 % pure, D_{50} = 23 µm), Si (Alfa Aesar, 99.5 % pure, D_{50} = 4 µm), Mg (Alfa Aesar, 99.8% pure, D_{50} = 62 µm), and prealloyed AlMg50 (Jagada Industries, 98 % pure, D_{50} = 37µm) powders were used to prepare AlSi13Mg5 (in wt%) alloy foam precursors. Note that AlMg50 contains 50 wt% of each element. The hydrogen release behaviour in Mg and AlMg50 powders was studied employing mass spectrometry in a Netzsch simultaneous thermal analyser STA 409C and 209F1 connected to a quadrupole mass spectrometer. For this, 100 mg of sample were heated from 30 °C to 600 °C with a heating rate of 10 K/min under argon atmosphere.

Two types of foamble precursors were prepared: one containing Mg powder and the other containing AlMg50 powder. Even though the same alloy was prepared, the amount of blowing agent added was different to maintain 5 wt% Mg in the composition. The precursor prepared using AlMg50 powder contained 77 wt% Al, 13 wt% Si, and 10 wt% AlMg50. And the precursor prepared using Mg powder contained 82 wt% Al, 13 wt% Si, and 5 wt% Mg. In this work, AlSi13Mg5 alloys/foams prepared using two different blowing agents (BA) are denoted using the following terminology. The AlSi13Mg5 alloy/foam produced using Mg powder as alloying element as well as the blowing agent will be referred to as 'BA-M' alloy/foam and the AlSi13Mg5 alloy/foam produced using AlMg50 powder as the blowing agent will be referred to as 'BA-AM' alloy/foam.

Powder blends were compacted by applying 500 MPa uniaxial pressure at 450 °C for 20 min. Compaction resulted in pellets with 36 mm diameter, which were machined to obtain 24 × 23 × 11 mm^3 samples for foaming. Foaming was performed on a pre-heated ceramic heating plate for 4 min at 800 °C, which corresponds to a sample foaming temperature of 720 °C, as determined separately by additional tests using a second thermocouple placed inside the sample. Subsequently, the foams were solidified by turning off heating. At least three foams of each type (BA-M and BA-AM) were produced and analysed.

For characterisations, foam samples with an average dimension of 23 × 23 × 17 mm^3 were prepared using an abrasive cutter. Foam density was calculated from these samples by considering their mass and geometric volume. Foam sections from three samples in each category were scanned using an optical scanner, and 2D image analysis of the sections were performed using the ImageJ software. Two/three sections from each foam sample were analysed. The analyses of all the eight/nine sections of a given foam category were combined to determine cell size and cell circularity distribution. Cell size and circularity distributions were fitted by appropriate function to extract mean cell diameter (D_{mean}) and mean circularity (C_{mean}), respectively.

To identify the phases present in the solidified foams, powder samples were drilled out from the solidified foams and were grinded to fine powders using mortar and pestle. These fine powders were analysed employing Cu K_{α} radiation for X-ray diffraction (XRD) in Bragg-Brentano geometry using Rigaku Miniflex 600 X-Ray Diffractometer. Compression testing of the foams was performed in a Zwick/Roell Z100 testing machine with a deformation rate of 1 mm/min. Micro Vickers hardness test (using a FALCON 603 FA hardness tester) were carried out on the cell walls of the foams by applying a load of 30 gf for 10 s

3. Results and discussion

Mass spectrometry data reveals that both Mg and AlMg50 powders contain hydrogen, as shown in **Fig. 1**. However, the hydrogen evolution behaviour is different. Onset temperature of gas release was found out by drawing tangents to the curve and it was found out to be 272 °C and 329 °C respectively for Mg and AlMg50 powders. **Fig. 1** shows that both peak initiation as well as peak gas release is later in the case of AlMg50 blowing agent. The peak gas release from Mg powder takes place earlier (364 °C) compared to that from AlMg50 powder (420 °C). It is well known that during foaming of aluminium alloys with higher solidus temperature the delay in gas release from blowing agent is ideal for creating a good porous structure [7,17]. Because of the delayed gas releases from AlMg50 powders, the gas loss prior to precursor melting is minimized. Consequently, the gas is used more effectively during foaming of BA-AM precursors.

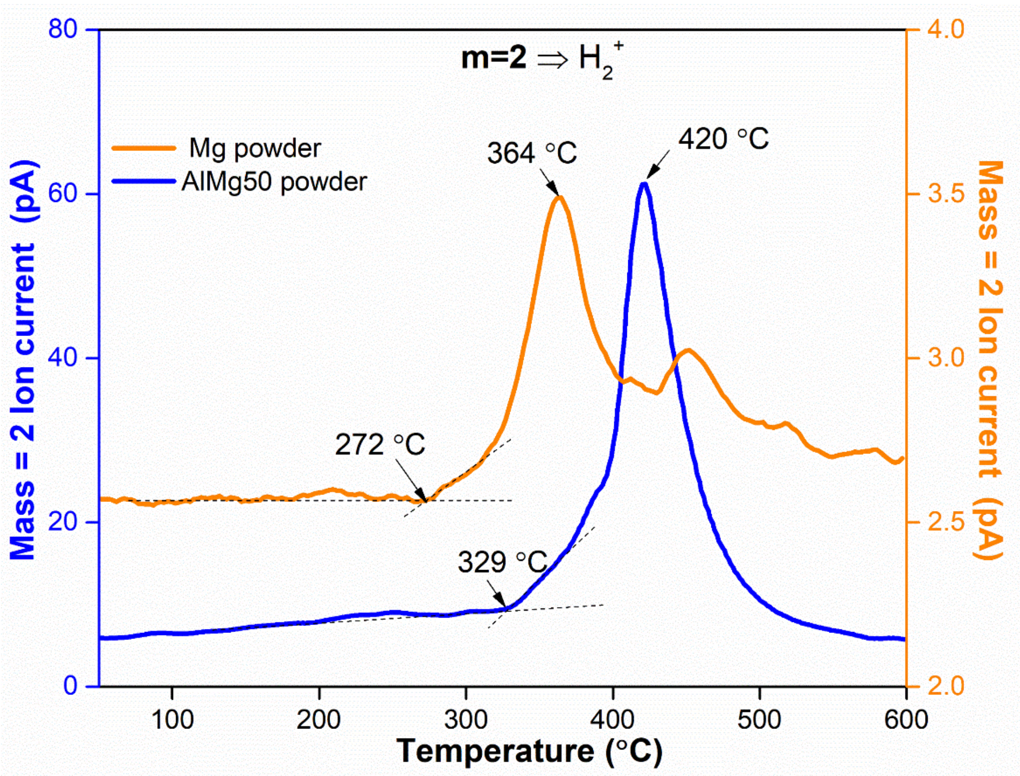

Fig. 1 Mass = 2 ion current corresponding to H_2^+, used as descriptor of the hydrogen release behaviour with respect to temperature for Mg and AlMg50 powders. Onset and peak temperatures of gas release are marked in the figure.

Both BA-M and BA-AM foams exhibit good porous structure and high expansion (nearly 20 % density), as seen in **Fig. 2**, and **Table 1**. An ONH analyser (LECO ONH 836 Analyser) was used to measure hydrogen content of these blowing agents. The hydrogen content was found to be 0.8 wt% and 0.2 wt% for Mg and AlMg50 powders, respectively. However, **Table 1** reveals that the foams produced using both blowing agents resulted in similar expansion. Even though AlMg50 powder contains only 0.2 wt% hydrogen, the effective hydrogen content is twice of this amount because 10 wt% AlMg50 powder was used for preparing BA-AM alloy precursors in contrast to 5 wt% Mg used for preparing BA-M alloy precursors. The amount of hydrogen available in these blowing agents is sufficient to achieve high expansion, as demonstrated in our previous study [14].

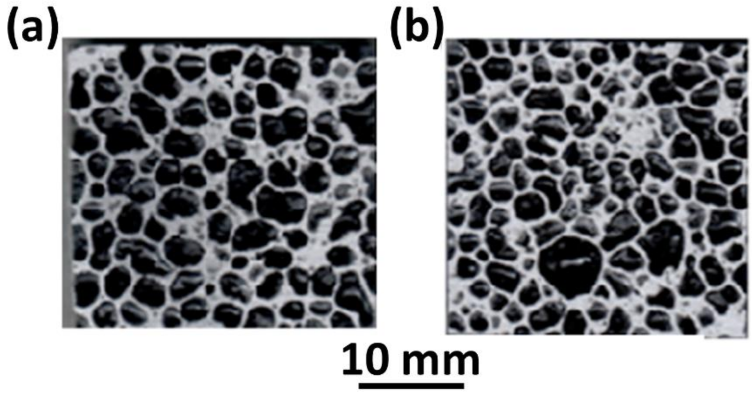

Fig. 2 Optical image of the representative section of the (a) BA-M foam and (b) BA-AM foam.

Table 1 Physical, structural and mechanical properties of the foams. Foam expansion and relative density were calculated from foam density data and the theoretical density (2.56 g/cm^3) of the AlSi13Mg5 alloy. The numbers mentioned within the brackets indicate the number of samples used to acquire the average data. Each hardness value is an average of 14 measurements (from two foam samples).

Foams	Structural and physical properties				Mechanical properties	
	D_{mean} (mm)	Density, ρ (g/cm^3)	Relative density, ρ_r	Expansion (%)	Hardness (HV0.3)	Peak strength (MPa)
BA-M foam	2.7 ± 0.9 (3)	0.55 ± 0.04 (3)	0.21 ± 0.02 (3)	370 ± 33 (3)	80.6 ± 9 (2)	7.3 ± 0.6 (3)
BA-AM foam	2.3 ± 0.7 (3)	0.56 ± 0.06 (5)	0.22 ± 0.02 (5)	363 ± 50 (5)	78 ± 7 (2)	8 ± 0.4 (3)

The structural analysis presented in **Fig. 3a** reveals slightly smaller D_{mean} (see **Table 1**) and a narrower cell size distribution in the case of BA-AM foams. Also, BA-M foams contain some large cells, for example, larger than 5 mm. These observations are in agreement with the one reported by Barode et al.: AlMg50 blowing agent results in smaller cell size compared to Mg blowing agent [12]. The amount of AlMg50 powder used is twice compared to Mg powder, as mentioned earlier. BA-AM alloy precursor may contain more pore nucleation sites compared to BA-M alloy precursors, thus resulting in a larger number of smaller cells in BA-AM foams [12]. Also, when AlMg50 powders are used, nucleation of pores initiates at the outer cell of these powders due to local melting of AlMg50 alloy (γ-$Al_{12}Mg_{17}$ phase, melting point 459 °C), which can convert to an even lower melting phase β-Al_3Mg_2 (melting point 450 °C) [18]. Such early and uniform nucleation of pores is ideal for creating smaller cells with narrow cell size distribution [11]. **Fig. 3b** shows that the circularity distribution of both types of foams is similar.

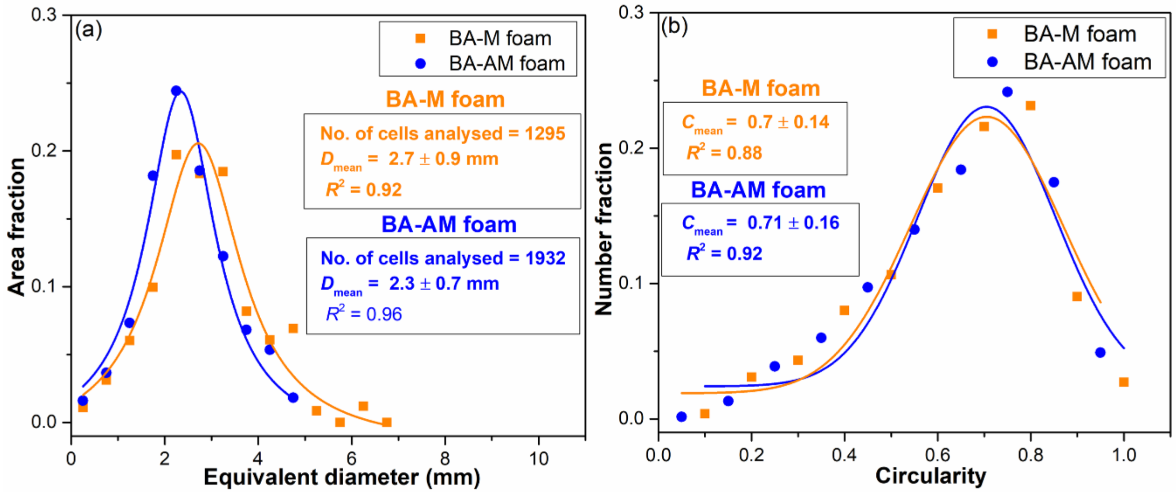

Fig. 3 (a) Cell size distribution of BA-M and BA-AM foams. The solid lines represent the fitting of the data by Gaussian function. (b) Number fraction as a function of circularity of the cells. The solid lines represent the fitting by Gaussian function. R^2 in both plots indicates the goodness of the fitting method used.

XRD analyses of the foams presented in **Fig. 4** reveals BA-M and BA-AM foams contain almost similar amount of Al, Mg_2Si, and Si phases, even though the source of Mg is different. This is expected because their microstructures are solidified microstructure from a fully molten state. Because of these reasons, all the phases are present in similar amount in both the foams. Consequently, the microstructural strength (yield strength) of BA-M and BA-AM foams is expected to be similar, which was confirmed by performing micro vickers hardness test. Indeed, BA-M and BA-AM foams possess similar hardness: 80.6 ± 9 and 78 ± 7, respectively.

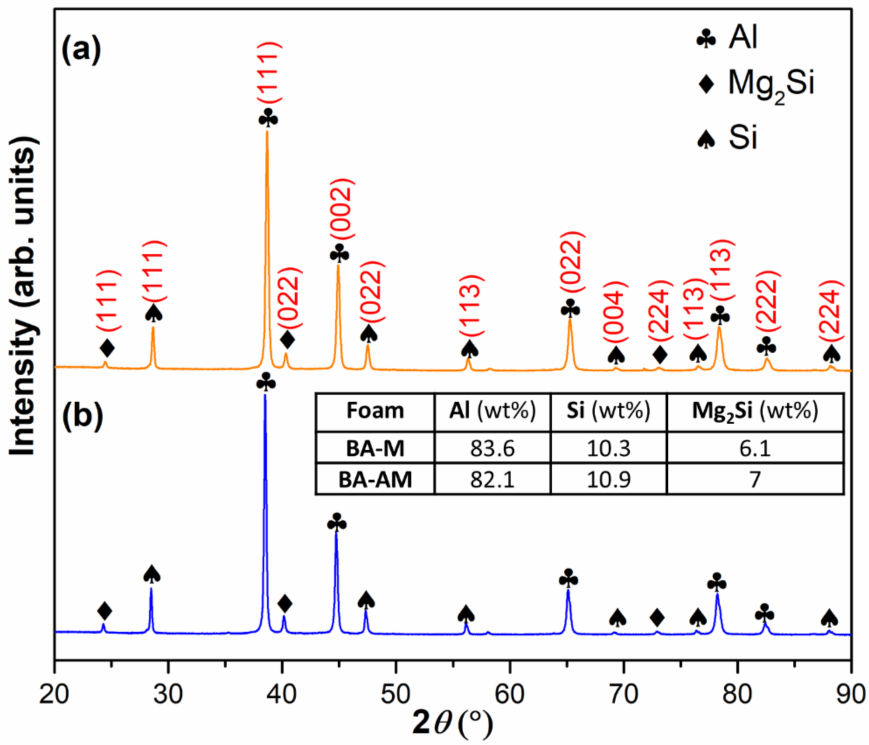

Fig. 4 XRD patterns of (a) BA-M foam and (b) BA-AM foam. Inset shows the quantitative analysis obtained using Rietveld refinement.

The peak strength was extracted from the stress-strain plots of the foams provided in **Fig. 5**. Both BA-M and BA-AM foams exhibited strain hardening behaviour. The serrations in the stress-strain curves of both foams indicate their brittle nature, which is because of the presence of brittle Si and Mg_2Si phases (see **Fig. 4**) in their microstructure [14,19]. The stress corresponding to the first peak in the stress-strain curve was taken as peak strength. **Table 1** shows that the average peak strength of BA-AM foams is higher than that of BA-M foams. Moreover, the deformation behaviour is more reproducible in the case of BA-AM foams.

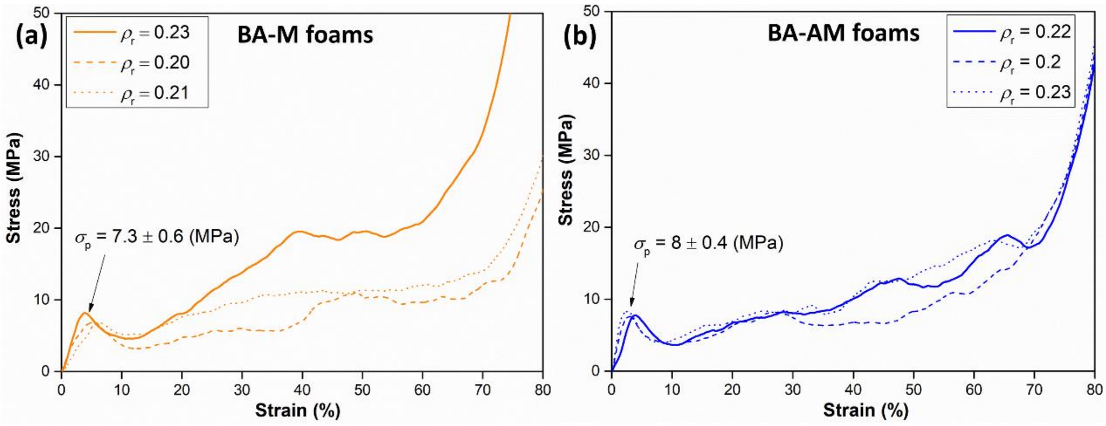

Fig. 5 Compressive behaviour of (a) BA-M foams and (b) BA-AM foams. The relative density (ρ_r) of the foams is mentioned in the legends.

Beside cell size, the shape of the cells also influences mechanical properties of the foams. For a given density, smaller cells offer higher strength because of their higher load bearing capacity [1,12,20]. Similarly, for given cell size, low circularity results in higher stress concentration thereby deteriorating the strength of the foam [20]. The circularity of cells is plotted as a function of cell size in **Fig. 6**, which reveals that the BA-M foams have larger cells with lower circularity, whereas larger cells in BA-AM foams are of higher circularity. The number contribution of cells having circularity greater than 0.8 is 12 % in the case of BA-M foams and 22 % in the case of BA-AM foams. In order to quantify the amount of large cells, a cell size twice the D_{mean} of BA-AM foam is considered. The area contribution from cells larger than 4.6 mm is 9 % in BA-M foams and 1.8 % in BA-AM foams. In summary, BA-M foams contain a higher amount of large cells with low circularity. Since both BA-M and BA-AM foams have similar density and microstructural strength, the improvement in the average peak strength of BA-AM foams compared to BA-M foams is attributed to the smaller cell size and cells with higher circularity of BA-AM foams. The narrow cell size distribution in BA-AM foams resulted in a more reproducible deformation behaviour, as seen in **Fig. 5**.

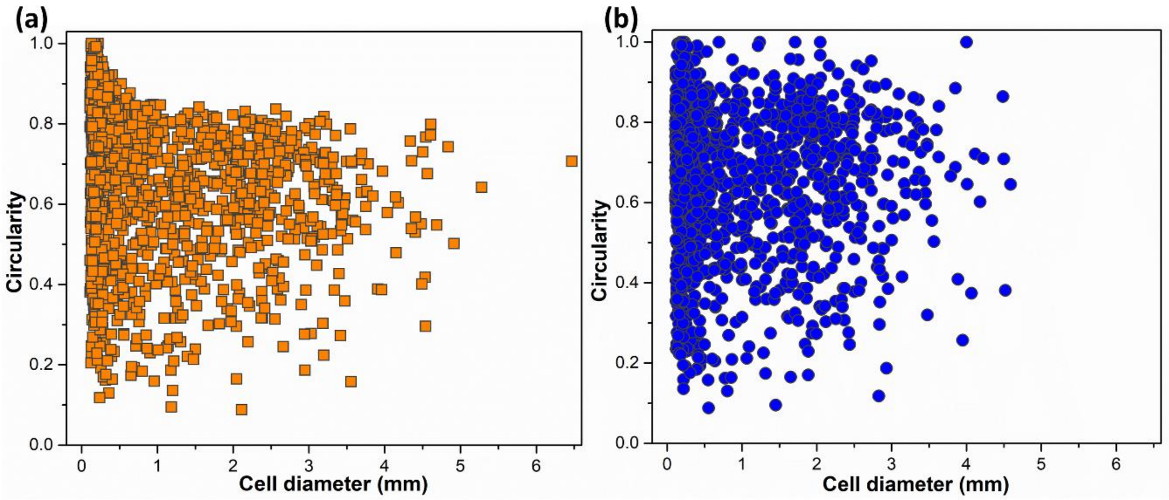

Fig. 6 Variation of circularity vs. cell diameter in (a) BA-M foams and (b) BA-AM foams.

4. Summary and outlook

AlSi13Mg5 alloy foams prepared using Mg and AlMg50 powders were compared. Mass spectrometry revealed that the hydrogen desorption characteristic is more favourable in the case of AlMg50 blowing agents. Compared to BA-M foams, BA-AM foams contain smaller cells with higher circularity, and therefore the average strength of BA-AM foams is higher than that of BA-M foams. BA-AM foams also exhibit a more producible stress-strain behaviour which could be because of their narrow cell size distribution. Therefore, it could be precisely concluded from this work that the AlSi13Mg5 foams produced using AlMg50 powder will result in at least similar properties, in case if it does not produce better properties than BA-M foams.

Between the two Mg-based blowing agents used in this study, elemental Mg powder is more expensive because of the difficulties associated with its production imposed by the high oxidation tendency of Mg. Therefore, besides having safety concerns, the usage of Mg powder as blowing agent implies a higher production cost, rendering it an unviable blowing agent for the commercial production of AlSi13Mg5 foams. Even though the properties of BA-M and

BA-AM foams are similar, the use of AlMg50 powder as blowing agent is therefore more cost-effective solution compared to the use of Mg powder as blowing agent.

Acknowledgement

The GK and MM acknowledge the funding received from the Ministry of Human Resource and Development for the Centre of Excellence (CoE) in Applied Magnesium Research (A Vertical of Centre for Materials and Manufacturing for Futuristic Mobility), IIT Madras (grant number SB20210992MEMHRD008517).

Conflict of interest statement

On behalf of all authors, the corresponding author states that there are no relevant financial or non-financial competing interests to report.

References

[1] F. García-Moreno, Commercial applications of metal foams: Their properties and production, Materials. 9 (2016) 20–24. https://doi.org/10.3390/ma9020085.

[2] G. Srinath, A. Vadiraj, G. Balachandran, S.N. Sahu, A.A. Gokhale, Characteristics of aluminium metal foam for automotive applications, Transactions of the Indian Institute of Metals. 63 (2010) 765–772. https://doi.org/https://doi.org/10.1007/s12666-010-0117-7.

[3] J. Banhart, Manufacture, characterisation and application of cellular metals and metal foams, Progress in Materials Science. 46 (2001) 559–632. https://doi.org/10.1016/S0079-6425(00)00002-5.

[4] T. Koizumi, K. Kido, K. Kita, K. Mikado, S. Gnyloskurenko, T. Nakamura, Foaming agents for powder metallurgy production of aluminum foam, Materials Transactions. 52 (2011) 728–733. https://doi.org/10.2320/matertrans.M2010401.

[5] J. Banhart, G.S. Vinod-kumar, P.H. Kamm, T.R. Neu, F. García-moreno, Light-metal foams : Some recent developments, Ciência & Tecnologia Dos Materiais. 28 (2017) 1–4. https://doi.org/https://doi.org/10.1016/j.ctmat.2016.06.002.

[6] B. Matijasevic, O. Görke, H. Schubert, J. Banhart, Zirconium hydride - a possible blowing agent for making aluminium alloy foams, Porous Metals and Metal Foaming Technology. (2006) 107–110.

[7] B. Muduli, T. Ramesh, K.C. Hari Kumar, N. Rajalakshmi, M. Mukherjee, Customised heat treatment of TiH_2 for the foaming of aluminium alloys, Materialia. 8 (2019). https://doi.org/10.1016/j.mtla.2019.100431.

[8] P.M. Proa-Flores, R.A.L. Drew, Production of aluminum foams with Ni-coated TiH_2 powder, Advanced Engineering Materials. 10 (2008) 830–834. https://doi.org/10.1002/adem.200800135.

[9] A. Azarniya, F. Salatin, M.R. Eskandaripoor, A. Rasooli, A kinetic study on the mechanism of hydrogen evolution in Ni-P coated titanium hydride powder, Advanced Powder Technology. 26 (2015) 259–266. https://doi.org/10.1016/j.apt.2014.10.007.

[10] V. Chilla, D.P. Mondal, G.D. Janaki Ram, M. Mukherjee, Thermal Expandometer : A device for monitoring in-situ foam filling of hollow profiles processed through powder metallurgy, Transactions of the Indian Institute of Metals. 73 (2020) 1837–1841. https://doi.org/10.1007/s12666-020-02000-z.

[11] M. Mukherjee, F. Garcia-Moreno, C. Jiménez, J. Banhart, Al and Zn foams blown by an intrinsic gas source, Advanced Engineering Materials. 12 (2010) 472–477. https://doi.org/10.1002/adem.201000017.

[12] J. Barode, U. Aravind, S. Bhogi, B. Muduli, M. Mukherjee, Mg and Mg-based

blowing agents for aluminium foam, Metallurgical and Materials Transactions B. 52 (2021) 292–304. https://doi.org/https://doi.org/10.1007/s11663-020-02008-2.

[13] K. Georgy, L. Neelakantan, K.C. Hari Kumar, M. Mukherjee, Influence of Cu, Zn and Si alloying elements on Al alloy foams produced using Mg blowing agent, Journal of Materials Science. 56 (2021) 2612–2630. https://doi.org/10.1007/s10853-020-05381-0.

[14] K. Georgy, K.C. Hari Kumar, M. Mukherjee, Optimization of Mg blowing agent content for foaming aluminum, Metallurgical and Materials Transactions B. 53 (2022) Metallurgical and Materials Transactions B. https://doi.org/10.1007/s11663-021-02403-3.

[15] A. Dudka, F. Garcia-Moreno, N. Wanderka, J. Banhart, Structure and distribution of oxides in aluminium foam, Acta Materialia. 56 (2008) 3990–4001. https://doi.org/10.1016/j.actamat.2008.04.040.

[16] K. Georgy, P. Banerjee, M. Mukherjee, The effect of heat treatment on the compression property of Al-Si-Mg foams produced using Mg blowing agent, Materials Today Communications. 36 (2023) 106445.

[17] A.R. Kennedy, The effect of TiH_2 heat treatment on gas release and foaming in Al - TiH_2 preforms, Scripta Materialia. 47 (2002) 763–767. https://doi.org/10.1016/S1359-6462(02)00281-6.

[18] P.H. Kamm, T. R. Neu, F. García-moreno, J. Banhart, Nucleation and growth of gas bubbles in AlSi8Mg4 foam investigated by X-ray tomoscopy, Acta Materialia. 206 (2021) 116583. https://doi.org/10.1016/j.actamat.2020.116583.

[19] M. Farahani, S.H. Elahi, Effect of Silicon content on mechanical properties and progressive collapse behavior of closed-cell aluminum foams, Transactions of the

Indian Institute of Metals. 74 (2021) 3145–3154. https://doi.org/10.1007/s12666-021-02390-8.

[20] K.S. Verma, D. Muchhala, S.K. Panthi, D.P. Mondal, Influences of cell size, cell wall thickness and cell circularity on the compressive responses of closed-cell aluminum foam and its FEA analysis, International Journal of Metalcasting. 16 (2022) 798–813. https://doi.org/10.1007/s40962-021-00627-2.